Fixed-bed Column Dynamics of Ultrasound and Na-functionalized Diatomite to Remove Phosphate from Water

Junxiu Ye (2427182426@qq.com)
Yunnan Minzu University
Min Yang
Yunnan Minzu University
Xuemei Ding
Yunnan Minzu University
Wei Tan
Yunnan Minzu University
Guizhen Li
Yunnan Minzu University
Shuju Fang
Yunnan Minzu University
Hongbin Wang
Yunnan Minzu University

Research Article

Keywords: Diatomite, modify, ultrasonic, sodium chloride, dynamic adsorption, Phosphate, Sewage treatment, Thomas model

Posted Date: April 13th, 2021

DOI: https://doi.org/10.21203/rs.3.rs-406797/v1

Version of Record: A version of this preprint was published at Environmental Science and Pollution Research on July 6th, 2021. See the published version at https://doi.org/10.1007/s11356-021-15126-4.

Fixed-bed column dynamics of ultrasound and Na-functionalized diatomite to remove phosphate from water

Junxiu Ye, Min Yang, Xuemei Ding, Wei Tan, Guizhen Li , Shuju Fang, Hongbin Wang*

School of Chemistry and Environment, Yunnan Minzu University, Kunming 650500, Yunnan, P.R. China

Corresponding author

Hongbin Wang, School of Chemistry and Environment, Yunnan Minzu University, Kunming 650500, Yunnan, China (E-mail: wanghb2152@126.com； Tel. +13708440749)

Abstract: A continuous fixed-bed column study has been used to evaluate phosphate adsorption performance of U-D-Na which was functionalized by the cheap NaCl reagent after simple ultrasonic purification of diatomite. Experimentally, various effect factors, the flow rate, the initial phosphate concentration， and the bed height on breakthrough time of fixed column were studied. Experimental results showed that the breakthrough time declined with the increase of inlet phosphorous concentration and feed rate, whereas the increase of bed height turned out to significantly prolong the breakthrough time. The dynamic adsorption data could better be fitted by the Thomas model, with the correlation coefficients obtained, R^2>0.9000 at the majority of operating conditions (5/7). At least thrice loop of adsorption and desorption was achieved with 0.1 M hydrochloric acid eluent and deionized water. The results proved that U-D-Na could be used as a better alternative phosphate adsorbent from wastewater in a continuous column process.

Key words: Diatomite; modify; ultrasonic; sodium chloride; dynamic adsorption; Phosphate; Sewage treatment; Thomas model

1. Introduction

Eutrophication caused by the high content of nutrients such as phosphate in water has always been concerning in the field of water treatment (Si et al. 2000). It was reported that the inland river basins in many developed countries (e.g. the United States) and some developing countries (e.g. China) were suffering from water eutrophication. And the trend of eutrophication is largely related to human activities; the level of pollution in the river nearby densely populated areas was more serious (Bhagowati &Ahamad 2018; Bu &Xu 2013; Yi et al. 2011). According to The U.S. Environmental Protection Agency (USEPA), the phosphate concentration in water exceeding 0.02 mg/L might lead to eutrophication. And China's "Pollutant Discharge Standard for Municipal Wastewater Treatment Plants" stipulated that the phosphate content in urban sewage discharge should be less than or equal to

0.50 mg/L. In recent years, in order to remove phosphate in sewage, plenty of operation methods, such as membrane filtration, adsorption, flocculation, precipitation, and crystallization had been carried out by many scholars (Duan et al. 2013; Fan et al. 2017; Greenlee et al. 2009; Wen &Jian 2008; Wu et al. 2018). Among these, the adsorption technology has been considered to be a potential option due to its simple operation, rapid adsorption performance, low cost, and high utilization rate of resources. This is of great significance in sewage treatment and environmental protection. (Cong et al. 2014; Zhao et al. 2018)

The adsorption technology has been widely applied to many water treatment plants for phosphate removal. This is an increasing tendency in fully utilizing effective adsorbent to remove target substances in sewage. Generally, the adsorbate is attached to the surface of the adsorbent due to a certain unbalanced attractive force, such as electrostatic attraction, chemical bonding, and van der Waals force. Meanwhile, most of the adsorption processes were accompanied by physical sedimentation. The strength of the acting force that existed in the adsorbent would largely affect the sorption performance. Therefore, the selection and optimization of the adsorbent have become a key factor in whether the technology can be applied to actual production. In the past few years, various adsorbents for phosphate removal had been reported by many scholars. such as the hydrated metal adsorbent reported (Chouyyok et al. 2010), in which HZrO and HFeO were dispersed into microporous of anion ion exchange resin (IRA-400); it was found that the removal rate for phosphate reached 83%. This might be because strong ligand sorption existed in poly-valent metals and phosphate. Furthermore, Zhou reported a novel adsorbent (LDHs) that was synthesized by a simple hydrothermal method, with the adsorption capacity reached 54.1 to 232mg/g (Zhou et al. 2011). At present, there are also several sporadic reports on the adsorption performance of diatomite at home and abroad.

The natural diatomite is an important silicate material evolved from seafloor diatoms. With a large number of micropores from surface to the interior, specific surface area, strong acid and alkali resistance, a lot of striking chemical and physical properties of diatomite have been observed. And the surface of diatomite was rich in silyl hydroxyl groups and hydrogen bonds (Xiao et al. 2010), which could cause a series of chemical reactions with particles. Many reaction mechanisms of diatomite were also based on those functional groups. According to the structural character of raw diatomite, a certain adsorption effect could be observed; moreover, modification of natural diatomite is a vital approach to realize its efficient adsorption. The majority of previous studies have been found that the functionalized

diatomite showed a promising sorption performance on phosphate ions. For instance, Xu and Pang pointed out that the phosphate removal efficiency of the diatomite could be largely improved by increasing the specific surface area, void volume of diatomite, and removing surface moisture and organic matter (Xu &Pang 2009). And also, a kind of diatomite modified by hydrated lanthanum chloride (La-diatomite) was reported (Wu et al. 2018) in which he demonstrated efficient phosphate adsorption, with the maximum adsorption capacity reaching 58.7 mg/g. Besides, it was also reported that a sizable high dephosphorization efficiency (close to 100%) could be achieved by diatomite functionalized with zeolite and aluminum metal modifier (Duan et al. 2013; Wu &Chen 2011) Numerous previous researchers had validated that the modified diatomite had an excellent sorption capacity; and some information of thermodynamics, kinetics, and adsorption mechanism had been obtained at the stage of static experiments. However, it is also extremely necessary for the researchers to carry out fixed-bed experiments to evaluate the practical performance of the novel adsorbent.

The column experiment was a continuous process of interaction between the target pollutant and the adsorbent. Many key factors such as initial concentration, feed rate, and bed depth that affect column efficiency need to be considered during the adsorption process. The large-scale sewage in industries was generally treated by fixed-bed adsorption. This process filled the gap that the static adsorption could only clean up small batches of solution (Singh et al. 2012). In the dynamic sorption test, with large amounts of target ions in the solution continuously enter and leave the column, the height of the saturation layer continuously increased while the height of the adsorption layer declined until the entire column almost lost its adsorption capacity that it reached the saturation state. The fixed-bed reached the above-mentioned saturation phase, which called the dynamic equilibrium. Indicators like breakthrough time, equilibrium adsorption capacity, and regeneration in the dynamic system are vital to evaluate the performance of columns. The dynamic sorption performance of an adsorbent could be measured by the breakthrough curves at different conditions. Generally, changes in flow rate and initial concentration would affect the mass transfer process of phosphate in the column, and further affecting the transfer rate and breakthrough time. According to previous researches, the feed rates, inlet concentrations, and bed heights were the main factors for breakthrough performance in fixed-bed experiments.

For those reasons, based on the static adsorption experiments of U-D-Na recently conducted by our research team, various test conditions were carried out to further explore the phosphate removal

ability in the fixed-bed column. We intend to draw conclusions from this research on the various influence factors of dynamic adsorption and regeneration experiment to provide some useful information for the design and operation of the U-D-Na on phosphate removal process from sewage in practical applications.

2 Materials and methods

2.1 Reagents and instruments

Natural diatomite used as the adsorbent precursor in this study was collected from the local province, Xundian, Yunnan, which could be developed for phosphate removal in water after simple modification treatment. In addition, the main chemicals such as KH_2PO_4 (GR), NaCl（GR）and HCl （AR ）were purchased from Tianjin Guangfu Fine Chemical Research Institute, Xilong Chemical Co. LTD and Tianjin Fengchuan Chemical Reagent Technology Co. LTD, respectively. The above reagents are prepared with secondary deionized water.

Electric heating blast drying oven DL402 and Ultrasonic cleaner AS10200AD produced by Tianjin Experimental Instrument Factory. The adsorbent was weighed by using the American Ohaus AR2140 electronic analytical balance. The anti-molybdenum antimony spectrophotometer 7200 was introduced in Uniko Shanghai Instrument Co.. LTD. Dynamic sorption experiments were operated in a fixed-bed column with an inside diameter of 0.8 cm and a bed height of 35 cm. A constant flow rate was guaranteed by a commercial peristaltic pump.

2.2 Experimental methods

2.2.1 Preparation of U-D-Na

The preparation methods of U-D-Na in this work can consult our research group's static adsorption experiment. Briefly, a proper amount of diatomite was crushed, screened and ultrasonic cleaned for 1 h, and keep them into the dry container after drying at 110 ℃. Mix the raw reagents treated above with 5% NaCl solution sufficiently for 2 hours, which was dried under 95 ℃ and preserved at 110 ℃. Finally, applying an adequate amount of diatomite in muffle furnace calcining at 400 ℃ for 2 hours, and then the adsorbent U-D-Na required was prepared successfully. (Specific details and data on the preparation of U-D-Na seeing the research group's unpublished paper attached in S.1.)

To acquire the microporous structure of adsorbent and its elementary composition, the U-D-Na was characterized by Scanning Electron Microscopy (SEM), Energy Disperse Spectroscopy

（EDS）. Microgram obtained from SEM could be seen that the surface micropores of U-D-Na were loosely arranged and ordered smoothly. Obviously, the sodium chloride flat attached diatomaceous earth surface and matched with the results on EDS. The result showed that sodium content in diatomite was increased after being functionalized. Relevant characterization data can be referred to support material S.1.

2.2.2 Dynamic adsorption experiment

The simple diagram of the fixed-bed column in the experiment was shown in Fig.1, and the column height was 35cm and inner diameter was 0.8cm. In the experiment, the peristaltic pump was used to transport the liquid and controlled the injection flow rate. A tank was placed at the outlet of the separation column to receive the tail liquid. In order to facilitate the connection between the column and peristaltic pump, and prevent the U-D-Na from floating; using suitable absorbent cotton to attach the steel sieve to the bottom of the column, and seal the top of the column with a ground-glass piston.

Firstly, a known quantity of U-D-Na was packed in the column to the desired bed height of 1, 3, and 5 cm (equivalent to 1.00, 3.00, and 5.00 g of U-D-Na); various concentrations of phosphate liquid (15.00, 20.00， and 25.00mg/L) were pumped into the column at the flow rate of 1.00, 2.00，and 3.00 mL/min, respectively. The effluent sample concentration was measured at the exit of the column by molybdenum antimony spectrophotometry (SEPA 1989) at a regular interval of 10 minutes.

2.2.3 Calculation of breakthrough curve parameters

The adsorption performance of a column generally could be evaluated by the breakthrough curve and the sorption capacity(Rout et al. 2017). The breakthrough curve was a function defined by the ratio of the outflow concentration C_t and the inlet concentration C_0 against time t. The breakthrough time (t_b) was determined as the time when the outlet phosphate concentration (C_t) reached 10% of the inlet phosphorus concentration (C_t / C_0 = 0.1). Similarly, the exhaustion time (t_s) was defined as the time when the outlet phosphorus concentration (C_t) reached 90% of the inlet phosphorus concentration (C_t / C_o = 0.9).

Calculation of total adsorption capacity ：

$$q_{total} = \frac{Q}{1000} * \int_{t=0}^{t=total} C_{ad} dt \quad (1)$$

Where，q_{total} is the total amount of phosphorous adsorbed onto U-D-Na column, mg/g; Q is volumetric flow rate, mL/min; C_{ad} is the difference in the phosphorus concentration at the initial time

and the t time caused by adsorption， mg/L； t_{total} is the total time for the column to reach saturation， min.

Calculation formula of equilibrium adsorption capacity ：

$$q_e = \frac{q_{total}}{M} \quad (2)$$

Where， q_e is the equilibrium uptake capacity, mg/g; Which is derived as the quantity adsorbed (q_{total}) per weight of adsorbent (M is the amount of U-D-Na packed in the column, g)

In addition to the total adsorption capacity and equilibrium adsorption capacity, the column adsorption capacity could also be evaluated by removal rate, which was calculated by dividing the difference between the initial concentration and equilibrium concentration of the solution by the initial concentration with formula as follows.

$$R(\%) = \frac{C_0 - C_t}{C_0} * \% \quad (3)$$

2.2.4 Theoretical model

It was essential to deeply understand the breakthrough performance of fixed-bed systems by appropriate mathematical models for the successful design and optimization of the adsorption process of packed columns. In actual operation, the variation of concentration of the column outlet with time and bed height could be evaluated and predicted by an appropriate mathematical model, which was convenient and necessary for expanding the experimental scale. Meanwhile, a suitable mathematical model could be also helpful for practitioners to know and explain the affinity, surface properties, and adsorption process between adsorbents and adsorbate (Foo et al. 2013). In the present research, to achieve the above objectives, the continuous adsorption process of U-D-Na was evaluated by using Thomas and Yoon-Nelson model.

2.2.5 Successive cycles of sorption and desorption by column

The experimental procedure of adsorption/desorption was conducted using HCl (0.10 mol/L) solution as eluent to assess the reusability of U-D-Na. In the process of operation, firstly, the phosphate solutions (25.00 mg/L) were passed through the fixed bed of 3g of U-D-Na at a constant flow rate (2 mL/min), at room temperature. Samples were collected after passing through the column to measure their concentrations at different time intervals. The adsorption experiment was terminated when the column reached saturation. At the first cycle, the column had reached saturation when the outflow phosphate ions were close to the initial concentration and then followed by 7.00% HCl and a moderate

volume of deionized water to pass through the column until the exit phosphate concentration was nearly equal to zero. The column then finished its regeneration and could be used for subsequent adsorption/desorption cycles experiments. Performing operations under the same condition three times repeatedly and measuring each phosphate removal rate of the column, and the regeneration capacity was obtained visually through the breakthrough curves.

3 Results and discussions

3.1 Study on dynamic adsorption using fixed-bed column

3.1.1 Effect of flow rate

Fig. 2 illustrated the breakthrough curves of the column packed with U-D-Na at various flow rates for an initial phosphate concentration of 25.00mgL and bed height of 3 cm. As can be seen from Fig. 2, the breakthrough time (50min, 30min, and 20min) and the exhaustion time (320, 110, and 90min) decreased with the increasing flow rates (1, 2, and 3 ml/min). Higher feed rates could result in a weaker interaction between the adsorbate molecules and adsorbent for the adsorption to be taken place (Dwivedi et al. 2008). A similar tendency was reported in Zhang's research (Zhang et al. 2014) that the activated laterite was used to remove phosphate. Also, the trends in the slopes of the breakthrough curves could be used to measure the sorption performance of the column. From Fig. 2, it was clear that the curves become steeper gradually with the flow rates increased, which indicated an excellent sorption capacity of the column at a higher feed rate. This is possibly due to a majority of active sites of U-D-Na were quickly occupied by massive phosphate ions available at a higher flow rate, urging them to get saturated more quickly. While the flow rate increased from 2 to 3 mL/min, the slope of curves was close to each other under those two conditions, the breakthrough curve did not change much. Therefore, a faster flow rate did not necessarily result in a sorption effect. A shorter breakthrough time and an exhaustion time at a higher flow rate were also reported elsewhere for sorption onto different adsorbent and adsorbate (Singh et al. 2012). The sorption capacity at different flow rates summarized in Table 1 showed a dropping trend with the uprising flow rates. It can be explained by a lower flow rate leading to more residence time of the phosphate ions in the column, longer contact occurred between phosphate ions and U-D-Na; the effective sorption interaction could be reached before phosphate ions flowed out of the column. Thus the higher adsorption capacity (1.43 mg/g) was observed at the lowest flow rate of 1 mL/min. Another possible explanation for the higher sorption capacity of U-D-Na was that those active sites with weaker affinity could be effectively captured by

phosphate ions in a lower flow, which agreed with the study (Bulgariu &Bulgariu 2013). Moreover, such performance at a higher flow rate was also one of the reasons for the earlier breakthrough and exhaustion time. Comprehensive analysis of breakthrough curves depicted in Fig. 2 and the experimental parameters from Table 1, the best sorption performance was obtained at the lowest flow rate (2 mL/min)

3.1.2 Effect of bed height

The breakthrough curves under various bed depths of 1, 3, and 5 cm were conducted under the initial concentration of 25.00 mg/L and a constant flow rate of 2 mL/min, the variation tendency was shown in Fig. 3. The amount of adsorbent in the column was approximately 1, 3, and 5 g, respectively. As can be seen from this graph, the breakthrough time (30 to 90 min) increased with the increasing bed height (1 to 5 cm). Likewise, the time requirement of phosphate solution for reaching saturation point was concomitantly increased with the growing bed height as expected. The exhaustion time listed in table 1 was 95, 110, and 280 min for the bed heights of 1, 3, and 5 g, respectively. This might be explained by the possibility of more binding sites available at taller bed heights for adsorption and leading to a higher MTZ (Jain et al. 2013). However, at a lower bed height, the diffusion of U-D-Na in the column was reduced due to the axial dispersion phenomenon (Vijayaraghavan et al. 2004). In addition, at greater depth, more surface area of adsorbent is available, which resulted in a large surface of active sites for sorption(Saha et al. 2012). Likewise, as depicted in table 1, the total phosphate uptake capacity (q_{total}) of U-D-Na was 2.15，2.78 and 6.63 g for the bed heights of 1, 3 and 5 cm, respectively, but the equilibrium adsorption capacity (q_e) was 2.15，0.93 and 1.33 mg/g, respectively. An obvious conclusion we could draw that q_e did not increase with the uprising q_{total}. Inversely, increasing the amount of U-D-Na from 1 to 5 g, q_e declined from 2.15 to 1.33 mg/g, which meant that the sorption capacity per gram weight adsorbent did not increase with the increase in bed height, and such sorption behavior was apparently attributed to the infinite phosphate ions in the column (Singh et al. 2012). However，it is found a positive correlation between the adsorption capacity and bed height (Kumar et al. 2011)，which could ensure the handling of large amounts of phosphate solutions.

3.1.3 Effect of influent phosphorus concentration

The influence of different inlet phosphate ions concentrations on the breakthrough curves at a given flow rate of 2 mL/min and bed depth of 3 cm was depicted in Fig. 4. The result indicated that the breakthrough time was reversely related to the influent phosphate concentration. The breakthrough

time was found to be 70, 60, and 30 min for the concentration of 15.00, 20.00, and 25.00 mg/L, respectively. As summarized in Table 1, a similar tendency was observed in exhaustion time (280, 190, and 110 min), which clearly decreased with a rise in initial phosphate concentration. Besides, the curves grew much steeper with a longer MTZ at a higher initial phosphate concentration. This might be ascribed to much more phosphate ions available at a higher concentration occupied those binding sites to be adsorbed. A lower concentration gradient could reduce the mass transfer coefficient or diffusion (Zhang et al. 2011). The steepness in the slope of the curves depicted in Fig. 4 showed an increasing uprise with the growing phosphate concentration. The steeper the curves, the better the sorption capacity of the column (Cruz-Olivares et al. 2013). A sharpness in slope indicated a shorter time for the column to reach saturation with a stronger adsorption rate. Nevertheless, the result in Table 1 illustrated that the equilibrium uptake (q_e) of U-D-Na for phosphate lightly fallen from 1.51 to 0.93 mg/g with the uprising phosphate inlet concentration from 15.00 to 25.00 mg/L. An uprising concentration did not significantly result in a considerable sorption capacity this study，reason behind this still needs to be explored. It can be merely inferred from the existing results that the increase in initial concentration mainly affects the adsorption rate and breakthrough time.

3.1.4 Analysis of experimental parameters

The effects of various parameters such as bed depth, initial phosphate concentration, and feed rate for breakthrough and exhaustion time of U-D-Na packaged fixed bed were discussed above. Similar to the findings of most researchers that the breakthrough and exhaustion time prolonged with the increase in bed height and feed rate, while decreased with the increasing initial concentration. This could be explained by the two aspects that (1) high concentration phosphate ions resulted in a lower mass transfer resistance ; (2) sufficient contact with abundant active sites was achieved per unit time during the adsorption process. Through a series of tests on the breakthrough time and adsorption capacity of the column packed with U-D-Na, the optimum sorption condition could be obtained at the feed rate of 2 ml/min, initial concentration of 25.00mg/L, and the bed depth of 3 cm. Follow-up experiments for column regeneration could be conducted in this condition.

3.2 Breakthrough curve model

3.2.1 Thomas model

The Thomas model was one of the most widely used models to evaluate column performance and predict the phosphate adsorption breakthrough curve(Foo et al. 2013). It was based on two

assumptions (1) the adsorption interface is not affected by chemical reaction with an absence of axial dispersion, and (2) data fits Langmuir isotherm and the second-order reversible reaction kinetics. Compared with the Adams-Bohart model, it was more suitable for describing the entire process of dynamic adsorption (C_t/ C_0 = 0-1)，), while the Adams-Bohart model was only suitable for describing the initial stage of the curve, namely the C_t/C_0 = 0-0.5, resulting in a limit of its validity in many ranges of conditions. The linear equation of the Thomas model and related symbols are shown below. Equilibrium adsorption capacity, q_0 and Thomas rate constant, K_{TH} were obtained by intercept and slope from the linear regression analysis of ln (C_0/C_t-1) against t, respectively.

$$\ln\left(\frac{C_0}{C_t}-1\right)=\frac{K_{TH}q_0m}{Q_0}-K_{TH}C_0t \quad (4)$$

Where, C_0 is the inlet phosphate concentrations, mg/L; C_t is the effluent phosphate concentrations, mg/L; q_0 is the adsorption capacity, mg/g; m is the mass of adsorbent, g; K_{TH} is the kinetic constant, mL/min.mg; Q_0 is the fed flow rate, mL/min.

The values of characteristic parameters of the Thomas model obtained from different experimental conditions were listed in Table 2. Thomas rate constant K_{TH} (0.70, 1.22, and 1.90 mL/min.mg) increased with the increase in feed rate from 1 to 3 mL/min, as the increase in initial phosphate concentration from 15.00 to 25.00mg/L, the value of K_{TH} increased from 0.80 to 1.22 mL/min.mg, whereas the sorption capacity, q_0 reduced from 1.53 to 1.34 mg/g. A larger value of K_{TH} was observed at a faster feed rate and a higher inlet concentration. This might be due to the larger concentration gradient and larger feed rate which could result in a higher driving force in this case. However, the K_{TH} was found reversely related to the bed height. This could be explained by the increase in bed height, namely an increase in the amount of adsorbent, leading to a large steric hindrance. A similar explanation was also reported (Paudyal et al. 2013). The equilibrium adsorption capacity, q_0 did not present a continuous variation trend at constant flow rates and bed heights in this experiment. In general, a rise both in flow rate and bed depth led to a q_0 value decrease. Analysis of the majority of data summarized in Table 2, Thomas model was found fitting well the dynamic sorption process of U-D-Na with the regression coefficient obtained R^2>0.9000 under most of the parameters (5/7). It could also be inferred that neither the internal nor the external diffusions of the adsorbent surface was the rate control step of the process (Chen et al. 2012). The predicted values (1.53, 1.19, and 1.34 mg/g) calculated by the Thomas model were shown in Table 2, which indicated a good agreement

300 with the experimental data (1.43, 0.93, and 1.13) at an uprising flow rate (1, 2, and 3 mL/min). Those
301 results validated that the Thomas model is suitable for representing the dynamic sorption process.

302 **3.2.2 Yoon–Nelson model**

303 Yoon-Nelson model, developed by Yoon and Nelson in 1981, is the simplest mathematical and
304 semiempirical expression with fewer parameters. This model need not consider the property of
305 adsorbent and physical characters of the column. Similar function with the Thomas model is suitable to
306 describe the whole process of dynamic adsorption. The Yoon–Nelson model was based on the
307 assumption: the rate of decrease in the probability of adsorption for each adsorbate molecule was
308 proportional to the probability of adsorbate and the probability of adsorbate breakthrough on the
309 adsorbent (Yoon &Nelson 1984). The Yoon–Nelson rate constant K_{YN} and the time reaching 50%
310 phosphorous breakthrough τ could be calculated from the linear plot of $\ln(\frac{C_t}{C_0-Ct})$ against t. The linear
311 expression of the Yoon–Nelson model was given by the following equation.

312 $$\ln\left(\frac{C_0}{C_0-C_t}\right) = K_{YN}t - \tau K_{YN} \quad (5)$$

313 Where, K_{YN} is the Yoon–Nelson rate constant (min^{-1}), and τ is the time required for 50%
314 phosphorous breakthrough (min).

315 The data obtained from Yoon-Nelson were listed in Table 2. It was found that the K_{YN} (0.0175,
316 0.0298, and 0.0426 min-1) increased while τ (184.58, 71.07, and 52.32 min) decreased with the flow
317 rate （1 to 3 mL/min）and initial concentration (15.00 to 25.00 mg/L) increased. A reasonable
318 explanation is that a faster time of τ could be reached at a higher flow rate and initial concentration.
319 A Similar tendency had been reported previously (Yuan et al. 2020). Nevertheless, a growth in bed
320 depth (1 to 5 cm) resulted in a fall trend in τ (158.67 to 71.07 min) and an uprising trend in K_{YN}
321 (0.0199 to 0.0298 min^{-1}). The results listed in Table 2 indicated that the flow rate had a huge effect on
322 τ, the value of τ decreased roughly three times, with the flow rate increased from 1 to 3 mL/min
323 when the sorption process was reaching 50% breakthrough point. According to the assumption of the
324 Yoon-Nelson model， it could be inferred that the probability of phosphate ions passing through the
325 column was enhanced at a higher flow rate. The correlation coefficient R^2 obtained from Yoon-Nelson
326 model was ranged from 0.8428 to 0.9519, under the majority of experimental conditions (5/7), the
327 values of R^2 were higher than 0.9000. However, the τ predicted values calculated by Yoon-Nelson did
328 not satisfactorily agree with the experimental values. At the flow rate of 1, 2, and 3 mL/min, the τ

predicted values were found to be 140.00, 52.00, and 50.00 min for the experimental values of 184.58, 71.07, and 52.32, respectively. The data gap between predicted and experimental values was listed in table 2, a conforming lower value in predicted than the experimental was observed under all of the conditions. Those results based on table 2 could be speculated that the Yoon-Nelson model neglect of axial dispersion is not suitable to describe the phosphate-U-D-Na sorption system.

3.2.3 Mathematical model analysis

In this experiment, the Thomas model and Yoon-Nelson model were used to fit the adsorption process of the phosphate-U-D-Na system. In comparison to Thomas and Yoon-Nelson model, the results given above validated that the Thomas model is more suitable to represent the sorption process of U-D-Na than the Yoon-Nelson model. As listed in Table 1, the values of R^2 obtained from the Thomas model ranged from 0.8482 to 0.9480, and under the majority of conditions (5/7) were higher than 0.9000. The q_e predicted values were found to be agreed well with those acquired from the experiment in the changes of flow rates and bed depths. On the other hand, the time for phosphate reaching 50% breakthrough, τ values predicted by Yoon-Nelson existed a large difference with the experimental values. At all the conditions, the values of τ were evidently lower than those obtained from experiments. The maximum absolute error among them was even reaching 57.67 min. These results demonstrated that the Yoon-Nelson model which ignored the properties of U-D-Na to describe the dynamic adsorption process is flawed.

3.3 Successive adsorption-desorption cycles

3.3.1 Regeneration of U-D-Na adsorbed phosphate.

In order to investigate the practical application ability of U-D-Na, the elution from a saturated bed was carried out with 7.00%HCl eluent at the same flow rate of 2 mL/min. The trend plot between the outlet concentration and the elution time was depicted in Fig. 5. It could be clearly seen from Fig.5 that with continuous addition of the eluent, the outlet phosphate concentration in the eluent represented a continuous declination. A sharp drop trend occurred in 60 min which indicated a large elution rate at this period. The outlet phosphate concentration was found to be 94.06 mg/L after a flow of dilute acid 7.00%HCl solution in 10 min, near four times higher than the initial concentration (25.00 mg/L), which indicated that the HCl solution could be considered as a highly effective eluent for phosphate ions in the batch system. Roughly 100 min the concentration of eluent could be reduced below 10% of the

initial elution concentration. A short regeneration time for the U-D-Na could be achieved. Besides, almost all phosphate ions attached to the column were cleared off within 180 min.

3.3.2 Breakthrough curves of the column after three times cycles

Fig. 6 depicted the breakthrough curves that the column of U-D-Na regenerated with HCl solution undergone three consecutive phosphate adsorption cycles to evaluate its reusability. It is clear that the breakthrough time did not change too much after being regenerated three times in the experiments. As depicted in Fig.6, along with the increase in cycle times (1, 2, and 3 cycles) of regeneration, the breakthrough time (30, 20, and 20 minutes) decreased slightly. However, the removal efficiency was almost unchanged, with similar high adsorption efficiencies for phosphate to the first two times. A declination in breakthrough time might be ascribed to the rupturing of certain binding sites， because part of the column damage was generated by those physical or chemical behavior in the adsorption/desorption process. According to the result of the breakthrough performance shown in Fig. 6, the U-D-Na was expected to be considered as a potential adsorbent because of its low-cost operation with an effective phosphate removal rate and resource-saving.

4. Conclusion

U-D-Na was found to be a promising candidate adsorbent for phosphate removal from the solution using a fixed-bed column in this study. The results showed that the breakthrough time was positively correlated with the bed height, but negatively correlated with the initial concentration and flow rate. Under the optimum experimental condition, the equilibrium sorption capacity (q_e) and the removal rate of U-D-Na for phosphate could reach 1.19 mg/g and 98.14%, respectively. The phosphate-U-D-Na sorption system was found well to be fitted by the Thomas model, with correlation coefficients, R^2>0.9000 under the majority of conditions (5/7), the surface sorption is the main rate-controlling step. Considerable removal efficiency after three desorption-adsorption cycles could near reach 98%. The effectiveness of continuous operations was evidenced successfully by the effective removal of phosphate from water onto the column. These results revealed that U-D-Na is an economical and environmentally friendly adsorbent for water treatment.

Declarations

Ethics approval and consent to participate

Not applicable.

Consent for publication

Not applicable.

Availability of data and materials

The datasets used and/or analyzed during the current study are available from the corresponding author on reasonable request.

Competing interests

The authors declare that they have no competing interests.

Funding information

This work was supported by the Science Research Fund Projects of Department of Education of Yunnan Province (Grant No. 2020J0329) and the Science Research Fund Projects of Department of Education of Yunnan Province (Grant No. 2020J0327)

Authors' Contributions

Funding acquisition, Wei Tan and Guizhen Li; methodology, Min Yang; experiment operation, Xuemei Ding and Junxiu Ye ; data curation, Xuemei Ding and Shuju Fang; writing—original draft, Junxiu Ye; writing—review and editing, Junxiu Ye, Guizhen Li and Hongbin Wang; All authors have read and agreed to the published version of the manuscript.

Acknowledgments

The main author sincerely acknowledges the Yunnan Minzu University for providing a good research platform. We all greatly thank professor Wang for providing a lot of valuable helps to guide our experiments. We would like to thank the anonymous reviewers and the editor.

Reference

Bhagowati B, Ahamad KU (2018) A review on lake eutrophication dynamics and recent developments in lake modeling. Ecohydrology and Hydrobiology, S164235931730143X. https://doi.org/10.1016/j.ecohyd.2018.03.002

Bu FP, Xu XY (2013) Planted floating bed performance in treatment of eutrophic river water. Environmental Monitoring & Assessment 185, 9651-9662. https://doi.org/10.1007/s10661-013-3280-6

Bulgariu D, Bulgariu L (2013) Sorption of Pb(II) onto a mixture of algae waste biomass and anion exchanger resin in a packed-bed column.Bioresource Technology 129, 374-380. https://doi.org/10.1016/j.biortech.2012.10.142

Chen SH, Yue QY, Gao BY et al (2012) Adsorption of hexavalent chromium from aqueous solution by modified corn stalk: A fixed-bed column study. Bioresource Technology 113, 114-120. https://doi.org/10.1016/j.biortech.2011.11.110

Chouyyok Wl, Wiacek RJ, Pattamakomsan K et al (2010) Phosphate Removal by Anion Binding on Functionalized Nanoporous Sorbents. Environmental Science & Technology 44, 3073-3078. https://doi.org/10.1021/es100787m

Cong HB, Mao ZL, Huang YL (2014) Study on the Phosphorus Removal Ability of Modified Calcite. Environmental Pollution & Control 36, 29-33+38. https://doi.org/10.15985/j.cnki.1001-3865.2014.10.034

Cruz-Olivares J, Pérez-Alonso C, Barrera-Díaz C et al (2013) Modeling of lead (II) biosorption by residue of allspice in a fixed-bed column. Chemical Engineering Journal 228, 21-27. https://doi.org/0.1016/j.cej.2013.04.101

Duan N, Zhang YF, Wu KM et al (2013) Preparation of diatomite composite adsorbent and its performance in removing nitrogen and phosphorus from wastewater. Bulletin of the Chinese Ceramic Society 32, 1528-1533. https://doi.org/10.16552/j.cnki.issn1001-1625.2013.08.041

Dwivedi CP, Sahu JN, Mohanty CR et al (2008) Column performance of granular activated carbon packed bed for Pb(II) removal. Journal of Hazardous Materials 156, 596-603. https://doi.org/10.1016/j.jhazmat.2007.12.097

Fan Y, Wang Z, Zhao LQ et al (2017) Study on the adsorption of phosphorus by zirconium modified diatomite. Environmental Science 38, 1490-1496. https://doi.org/10.13227/j.hjkx.201609132

Foo KY, Lee LK, Hameed BH (2013) Preparation of tamarind fruit seed activated carbon by microwave heating for the adsorptive treatment of landfill leachate: A laboratory column evaluation. Bioresour Technol 133, 599-605. https://doi.org/10.1016/j.biortech.2013.01.097

Greenlee LF, Lawler DF, Freeman BD et al (2009) Reverse osmosis desalination: Water sources, technology, and today's challenges. Water Research 43. https://doi.org/10.1016/j.watres.2009.03.010

Jain M, Garg VK, Kadirvelu K (2013) Cadmium(II) sorption and desorption in a fixed bed column using sunflower waste carbon calcium–alginate beads. Bioresource Technology 129. https://doi.org/10.1016/j.biortech.2012.11.036

446 Kumar R, Bhatia D, Singh R et al (2011) Sorption of heavy metals from electroplating effluent using
447 immobilized biomass Trichoderma viride in a continuous packed-bed column. International
448 Biodeterioration & Biodegradation 65, 1133-1139. https://doi.org/10.1016/j.ibiod.2011.09.003
449 Paudyal H, Pangeni B, Inoue K et al (2013) Adsorptive removal of fluoride from aqueous medium using
450 a fixed bed column packed with Zr(IV) loaded dried orange juice residue. Bioresour Technol 146,
451 713-720. https://doi.org/10.1016/j.biortech.2013.07.014
452 Rout PR, Bhunia P, Dash RR (2017) Evaluation of kinetic and statistical models for predicting
453 breakthrough curves of phosphate removal using dolochar-packed columns. Journal of Water
454 Process Engineering 17. https://doi.org/10.1016/j.jwpe.2017.04.003
455 Saha PD, Chowdhury S, Mondal M et al (2012) Biosorption of Direct Red 28 (Congo Red) from
456 Aqueous Solutions by Eggshells: Batch and Column Studies. Separation Science & Technology 47,
457 112-123. https://doi.org/10.1080/01496395.2011.610397
458 SEPA (1989) Water and wastewater monitoring and analysis methods. China Environmental Science
459 Press
460 Si YB, Wang SQ, Chen HM (2000) Loss of nitrogen and phosphorus in farmland and eutrophication of
461 water body. Soils 32, 188-188. https://doi.org/10.13758/j.cnki.tr.2000.04.005
462 Singh A, Kumar D, Gaur JP (2012) Continuous metal removal from solution and industrial effluents
463 using Spirogyra biomass-packed column reactor. Water Research 46, 779-788.
464 https://doi.org/10.1016/j.watres.2011.11.050
465 Vijayaraghavan K, Jegan J, Palanivelu K et al (2004): Removal of nickel(II) ions from aqueous solution
466 using crab shell particles in a packed bed up-flow column. Journal of Hazardous Materials 113,
467 223-230. https://doi.org/10.1016/j.jhazmat.2004.06.014
468 Wen HX, Jian P (2008) Development and characterization of ferrihydrite-modified diatomite as a
469 phosphorus adsorbent. Water Research 42. https://doi.org/10.1016/j.watres.2008.09.030
470 Wu L, Chen YF (2011) Study on Modified Diatomite for Dephosphorization of Chaohu Lake Water.
471 Chinese Journal of Environmental Engineering 5, 777-782.
472 https://doi.org/10.3724/SP.J.1011.2011.00468
473 Wu Y, Li XM, Yang Q (2018) Hydrated lanthanum oxide-modified diatomite as highly efficient
474 adsorbent for low-concentration phosphate removal from secondary effluents. Journal of
475 environmental management. https://doi.org/10.1016/j.jenvman.2018.10.059

476 Xiao LG, Zhao Z, Yu WZ (2010) Development status and prospect of diatomite at home and abroad.
477 Journal of Jilin Jianzhu University 27, 26-30. https://doi.org/CNKI:SUN:JLJZ.0.2010-02-008
478 Xu RR, Pang WQ (2009) Inorganic Synthesis and Preparative Chemistry. Higher Education Press.
479 https://doi.org/10.3321/j.issn:1005-281X.2000.04.011
480 Yi LL, Jiao WT, Chen XN et al (2011) An overview of reclaimed water reuse in China. Journal of
481 Environmental Sciences 23, 1585-1593. https://doi.org/10.1016/S1001-0742(10)60627-4
482 Yoon YH, Nelson JH (1984) Application of Gas Adsorption Kinetics I. A Theoretical Model for
483 Respirator Cartridge Service Life. Am Ind Hyg Assoc J 45, 517-524.
484 https://doi.org/10.1080/15298668491400205
485 Yuan L, Chen Y, Liu M et al (2020) Dynamic adsorption and regeneration of phosphorus by modified
486 nano-cellulose. Chemical Industry and Engineering Progress 39, 2907-2914.
487 https://doi.org/10.16085/j.issn.1000-6613.2019-1757
488 Zhang L, Wu WT, Liu JY et al (2014) Removal of phosphate from water using raw and activated laterite:
489 batch and column studies. Desalination & Water Treatment 52, 778-783.
490 https://doi.org/10.1080/19443994.2013.826786
491 Zhang WX, Dong L, Yan H et al (2011) Removal of methylene blue from aqueous solutions by straw
492 based adsorbent in a fixed-bed column. Chemical Engineering Journal 173, 429-436.
493 https://doi.org/10.1016/j.cej.2011.08.001
494 Zhao YF, Su X, Zhang WH et al (2018) Study on the adsorption of phosphorous wastewater by modified
495 diatomite. Applied Chemical Industry 47, 883-886.
496 https://doi.org/10.16581/j.cnki.issn1671-3206.20180330.083
497 Zhou JB, Yang SL, Yu JG et al (2011) Novel hollow microspheres of hierarchical zinc-aluminum
498 layered double hydroxides and their enhanced adsorption capacity for phosphate in water. Journal
499 of Hazardous Materials 192, 1114-1121. https://doi.org/10.1016/j.jhazmat.2011.06.013
500

Figures

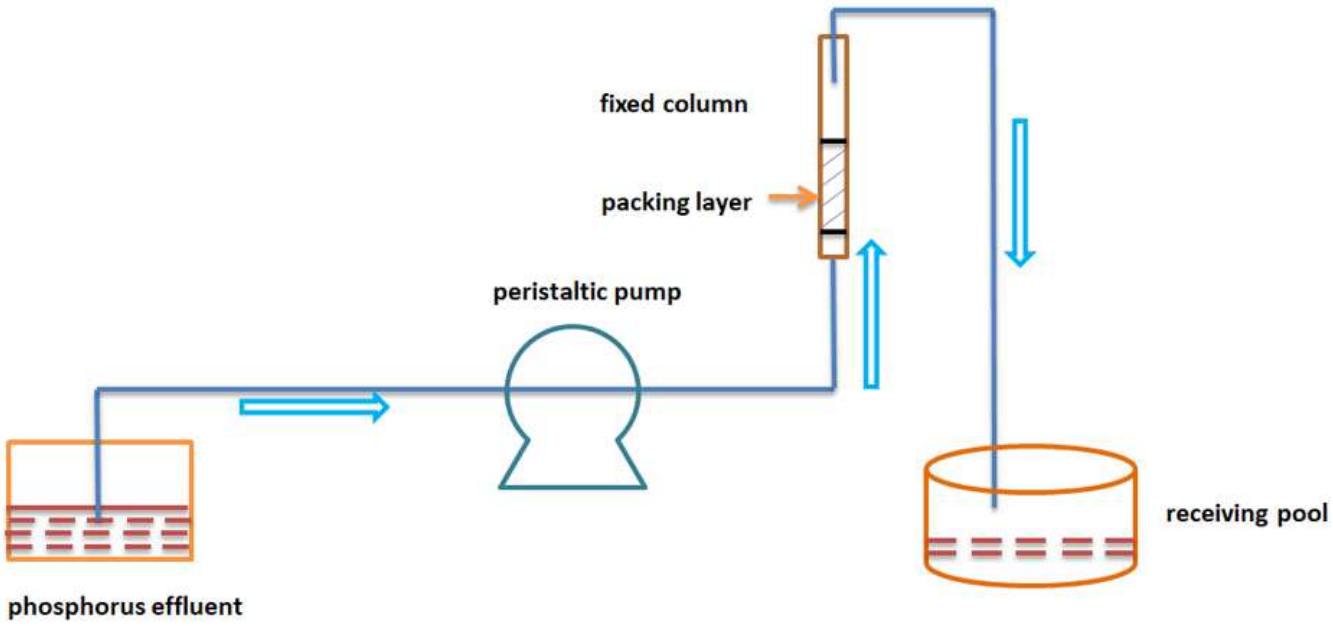

Figure 1

Simple diagram of phosphorus removal experimental apparatus

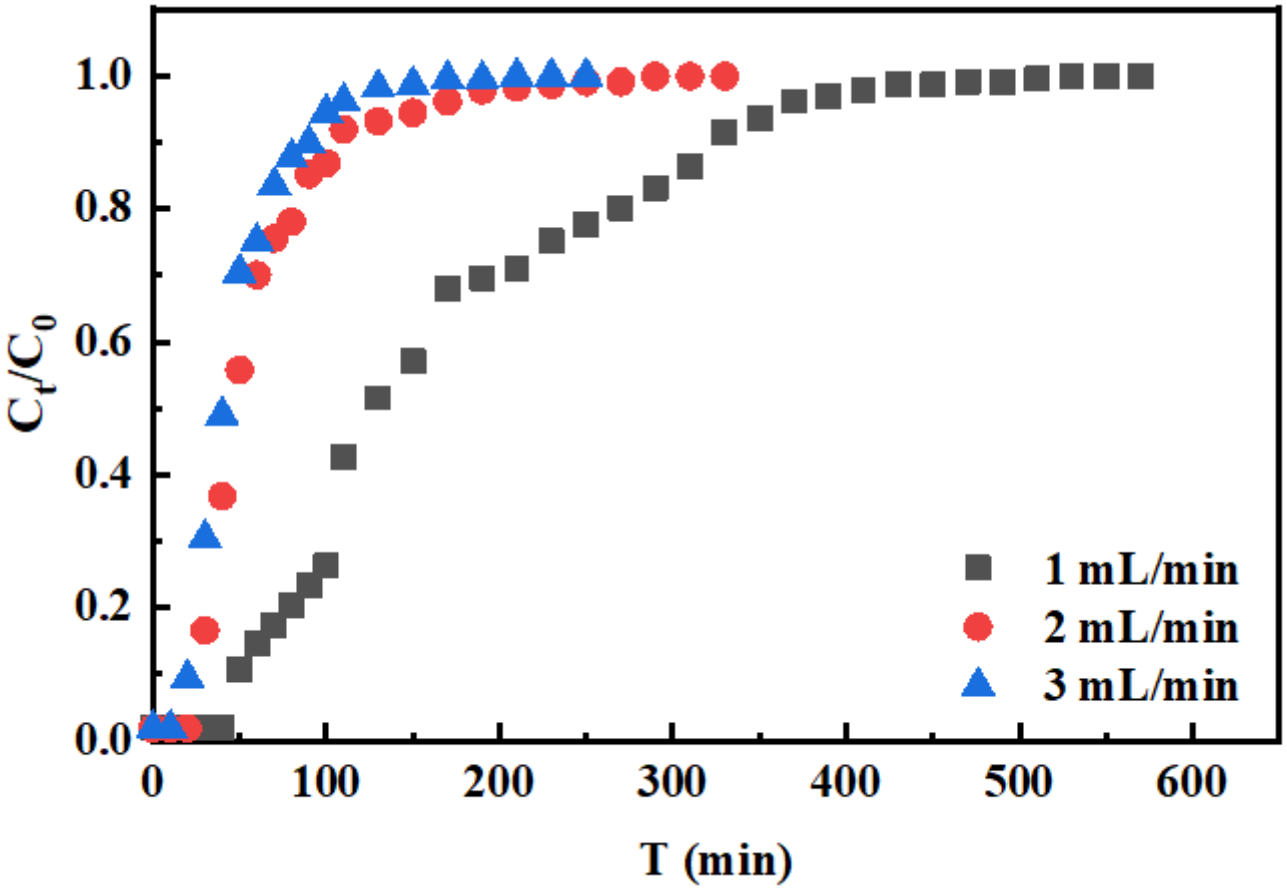

Figure 2

Effect of flow rate on the breakthrough curve of phosphate adsorption onto U-D-Na (natural pH, initial phosphate concentration of 25 mg/L, bed height of 3 cm)

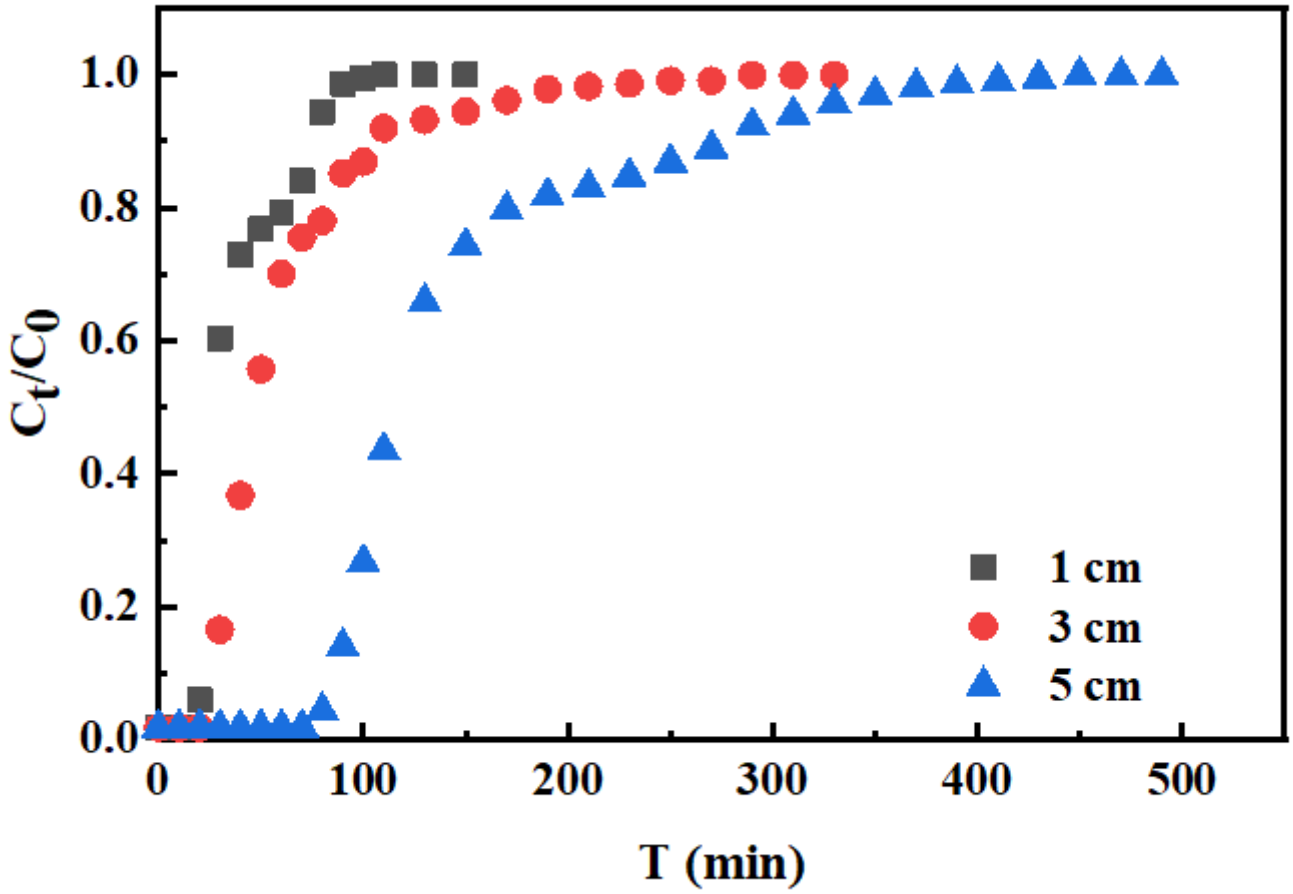

Figure 3

Effect of bed height on the breakthrough curve of phosphate adsorption onto U-D-Na (natural pH, flow rate of 2 mL/min, initial phosphate concentration of 25 mg/L)

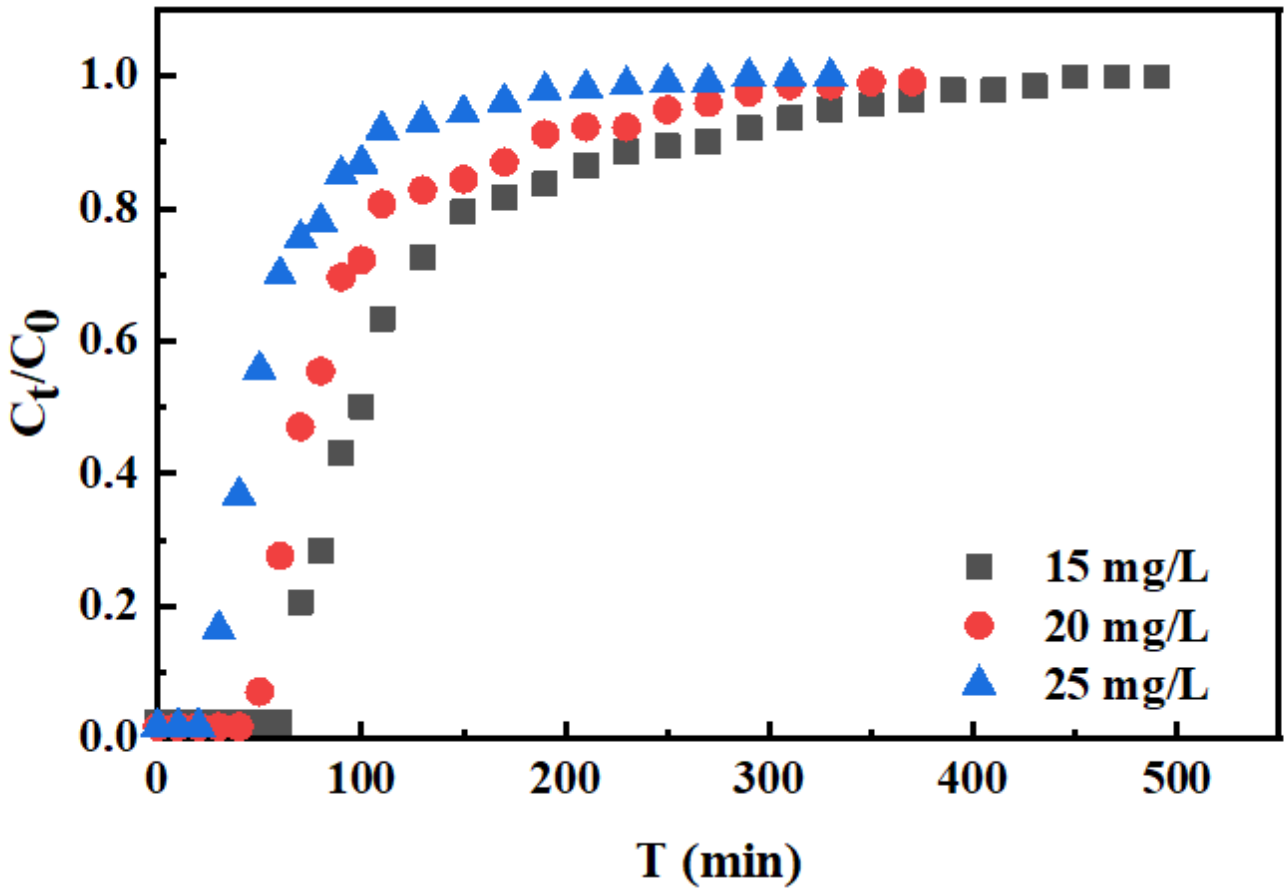

Figure 4

Effect of influent phosphorus concentration on the breakthrough curve of phosphate adsorption onto U-D-Na (natural pH, flow rate of 2 mL/min, bed height of 3 cm)

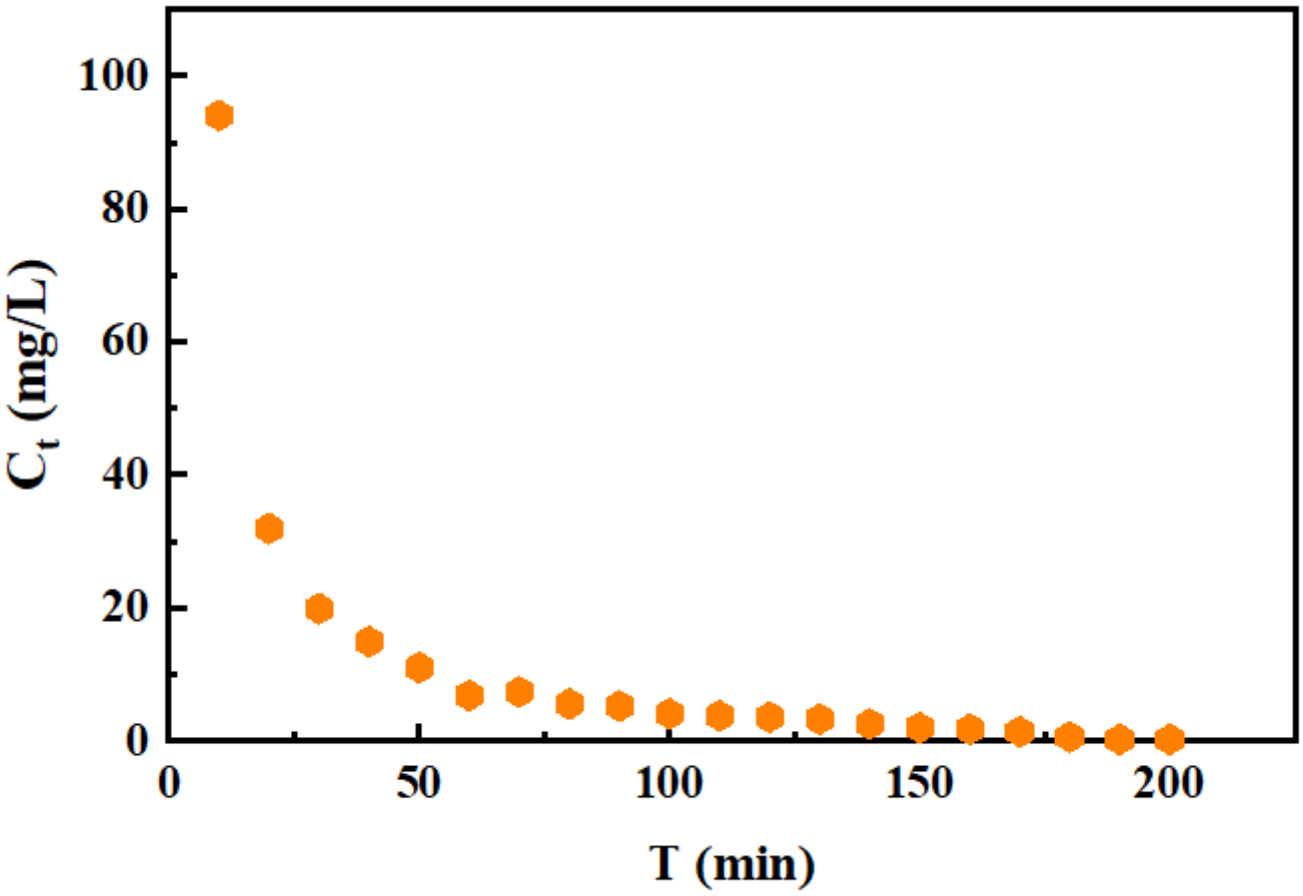

Figure 5

Change of solution concentration with elution time (Eluent of 7.00%HCl, flow rate of 2.00ml/min)

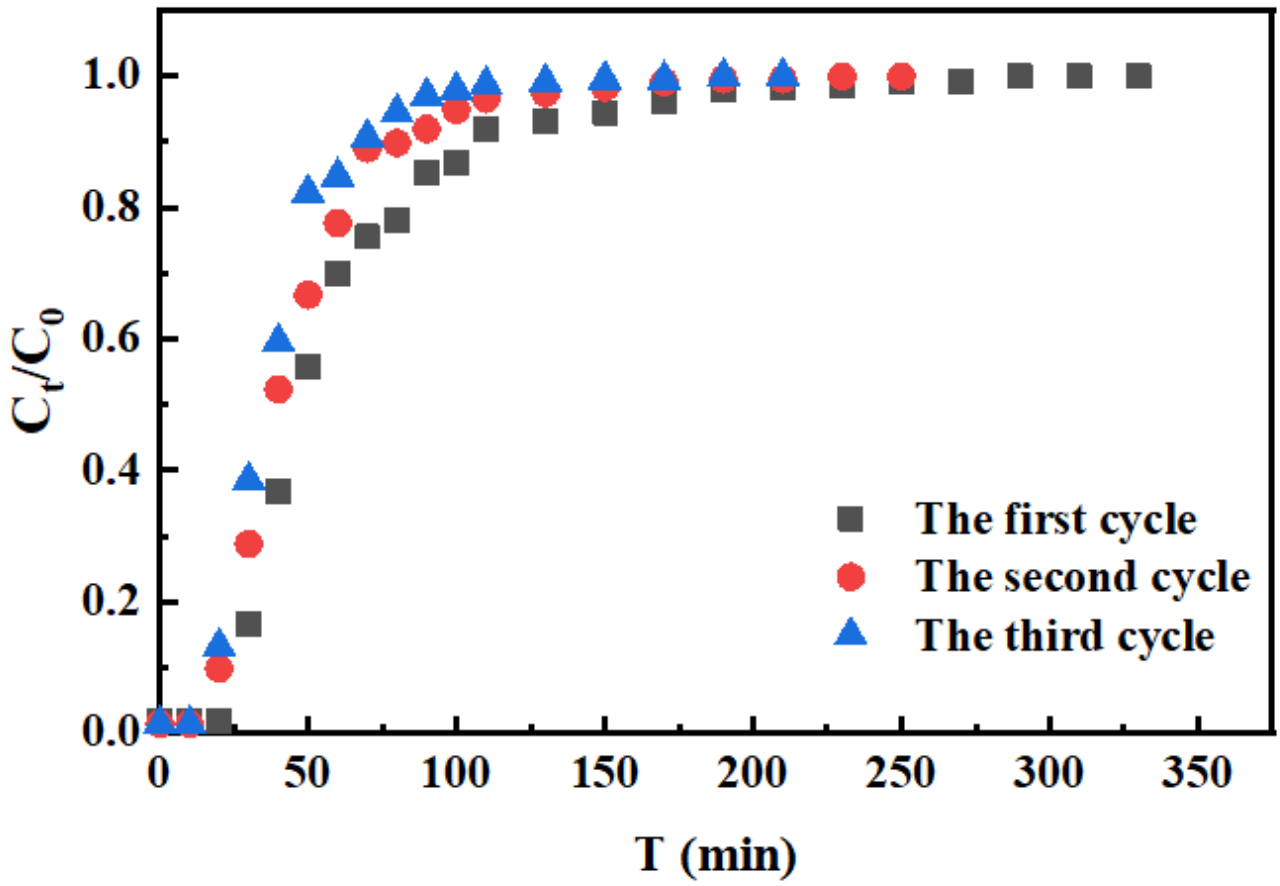

Figure 6

Influence of the number of regenerations in the column on the breakthrough time

Supplementary Files

This is a list of supplementary files associated with this preprint. Click to download.

- SupplementaryMaterials.docx